Mineralogical Magazine, December 2012, Vol. 76(8), pp. 3045–3053

Calcium silicate hydrate (C-S-H) gel dissolution and pH buffering in a cementitious near field

G. M. N. Baston, A. P. Clacher, T. G. Heath*, F. M. I. Hunter, V. Smith and S. W. Swanton

AMEC, Building 150, Thomson Avenue, Harwell, Didcot, Oxfordshire, OX11 0QB

[*Received 8 January 2012; Accepted 2 July 2012; Associate Editor: Nicholas Evans*]

ABSTRACT

A cementitious backfill has been proposed in many geological disposal concepts for intermediate-level waste and low-level waste in the UK and elsewhere. In this paper, the main features of the chemical evolution of backfill and the associated changes in the near-field pH are illustrated with results from recent work. For example, interaction of the groundwater with calcium silicate hydrate (C-S-H) phases in a backfill is expected to play an important role in the long-term pH-buffering behaviour. Existing experimental data for the dissolution of C-S-H gels are compared with recent experimental results from leach tests on gels of a lower calcium to silicon ratio (C/S) to provide a consistent set of data across the full C/S range. The results confirm that a congruent dissolution point around C/S = 0.8 is approached by leaching from below (i.e. for gels with $0.29 < C/S < 0.8$), as well as from above, as reported elsewhere. In addition, a spreadsheet model has been developed to calculate the volume of backfill required at the vault scale to meet specified pH performance criteria. This model includes the major reactions of the backfill with the groundwater, waste encapsulants and waste components. It can also consider the effects of specific waste packages on local pH performance to allow comparison with the vault-scale calculations.

Keywords: evolution, near-field performance, backfill, engineered barrier, calcium silicate hydrate, C-S-H gels, disposal concept.

Introduction

A cementitious backfill has been proposed in many geological disposal concepts for intermediate-level waste (ILW) and low-level waste (LLW) in the UK and elsewhere (Nuclear Decommissioning Authority, 2010*b*). One of the main safety functions of such backfills is to provide predictable controls on the near-field chemistry, including the maintenance of alkaline, low-carbonate conditions. Under such conditions the solubility of some key radionuclides is greatly reduced, lowering their rates of dissolution into the porewater and their release from the near field.

The evolution and duration of the chemical conditioning provided by the backfill depends on a wide range of processes that arise from the curing of the backfill, and its interactions with the groundwater and waste forms. Understanding these processes is fundamental in justifying: (1) arguments underlying the disposal system safety case for cementitious disposal concepts; and (2) assumptions concerning the ranges of chemical conditions applied in selecting chemical data for use in post-closure performance assessment calculations.

The cementitious concept in the UK includes a requirement for the maintenance of high pH conditions. In performance assessments, carried out in support of safety cases for this concept in the UK (Nuclear Decommissioning Authority, 2010*a*), the pH of the near-field porewater (as measured at 25ºC) is assumed to be maintained at

* E-mail: tim.heath@amec.com
DOI: 10.1180/minmag.2012.076.8.20

© *2012 by AMEC. All rights reserved. This article may not be reproduced or used in any manner whatsoever (except for the sponsors of the work) without the express written permission of the author.*

a value above pH 9 for a period of at least one million years. An understanding of the processes affecting pH underpins this assumption.

pH evolution

As groundwater enters the near field, it will be conditioned to a high pH as it dissolves the alkali oxides, and equilibrates with the cementitious phases in the backfill (such as portlandite, $Ca(OH)_2(s)$, and calcium silicate hydrates, C-S-H). Over time, leaching of the backfill by the groundwater will reduce its alkaline buffering capacity and eventually decrease the pH of the near field towards that of a groundwater. Leaching experiments and modelling studies have allowed an overall picture of the stages in the long-term pH evolution to be developed. These stages are summarized in Fig. 1, following Wang *et al.* (2009).

Modelling of cementitious backfill interactions

Modelling of the chemical interaction of cementitious backfill materials with a wide range of waste components and groundwater elements has progressed in recent years. Studies related to UK disposal concepts include the development of a relatively simple spreadsheet model for assessing backfill requirements. This allows a wide range of reactions with waste components to be included and is described below. For detailed investigation of the evolution of the cement mineralogy (including incongruent C-S-H dissolution), and the effects on the spatial variation of mineral phases in and around packages, a reactive transport model has been developed. This modelling applied the *TOUGHREACT* computer program to allow the effects of dissolution and precipitation on porosity and flow to be accurately represented (Hoch *et al*., 2009, 2012).

pH buffering by C-S-H phases

Calcium silicate hydrate phases are expected to play a crucial role in buffering the pH of the near-field porewater, once any $Ca(OH)_2(s)$ in the backfill is exhausted. Experimental studies have shown that progressive leaching in deionized water leads to incongruent dissolution of C-S-H gels (Fig. 2). For systems of high initial calcium/silicon molar ratio (C/S), preferential leaching of calcium (compared to silicon) occurs until C/S decreases to around 0.8. The C-S-H gels then dissolve congruently (Harris *et al*., 2002). Current research is extending these studies to investigate: (1) the leaching behaviour of low calcium C-S-H gels (initial C/S up to 0.6, these data are shown as filled symbols in Fig. 2); (2) the associated structural changes to the C-S-H gels (using X-ray diffraction); (3) the applicability of ideal solid solution models to these systems.

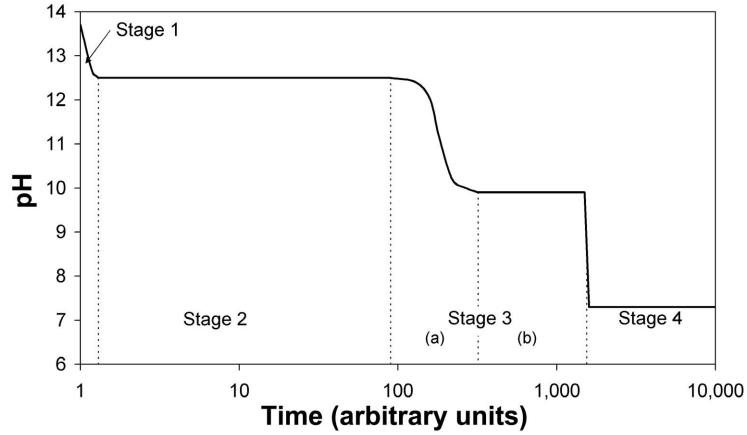

FIG. 1. Schematic representation of near-field pH evolution: stage 1: pH >12.5 due to dissolution of sodium and potassium oxides; stage 2: pH ~12.5 buffered by $Ca(OH)_2(s)$ component of the backfill; stage 3a: pH falling from 12.5 to ~9.8 controlled by the incongruent dissolution of C-S-H phases; stage 3b: pH ~9.8 controlled by congruent dissolution of C-S-H phases (or secondary mineral phases); stage 4: pH <9 determined by the groundwater and phases such as calcite; cementitious phases exhausted; based on reported diagram (Wang *et al*., 2009).

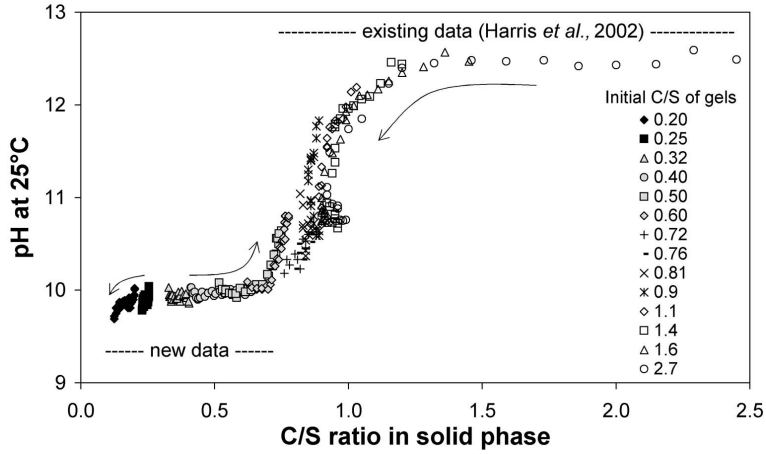

FIG. 2. Dynamic leach test results for C-S-H gels of varying initial C/S; arrows indicate evolution of solid composition during successive equilibrations with deionized water.

Experimental methodology

Calcium silicate hydrate gels of low C/S were prepared by methods similar to those employed previously to prepare C-S-H gels of higher C/S (Chambers *et al.*, 2003; Swanton *et al*,. 2004). Batches of C-S-H gel at six target C/S values of 0.20, 0.25, 0.32, 0.40, 0.50 and 0.60, were prepared as slurries by dispersing the required amount of analytical grade calcium oxide in a known volume of nitrogen-sparged demineralized water, to which was added an appropriate amount of colloidal silica dispersion to give the required C/S. Gels were prepared in a nitrogen-atmosphere glovebox. The containers were sealed and shaken vigorously as the gels began to form. The gels were left to cure for one month with regular shaking to ensure that they did not solidify.

After curing, portions of slurry were dried to constant weight at 80ºC for 6 days then at 105ºC within the nitrogen-atmosphere glovebox to determine the dry solid content of each batch. Additional samples were dried to constant weight over silica gel at ambient temperature to determine the bound water content of the gels. In each case, samples were centrifuged to separate the bulk of the free water, which was removed, before drying. Combined samples of the free water from each batch were filtered through 0.45 μm filters (pre-conditioned with water and C-S-H gel equilibrated water) to obtain samples of the equilibrated water for initial pH measurement and for inductively coupled plasma atomic emission spectroscopy (ICP-AES) analysis for calcium and silicon. Samples of the dried gels were taken to the University of Sheffield for examination by X-ray diffraction (XRD).

Leaching of the gels was carried out in duplicate for each target C/S value. A known weight of well mixed C-S-H gel slurry was added to the experimental container, to which was then added nitrogen-sparged demineralized water to give a solid to liquid ratio of 4 g of C-S-H gel to 600 cm^3 water. The containers were mixed and then sealed, removed from the glovebox and immersed in a thermostatically controlled water bath maintained at 25±1ºC. After a minimum of 11 days, 480 to 500 cm^3 of supernatant leachate were carefully decanted and replaced by an equivalent volume of nitrogen-sparged demineralized water. The pH of the leachate removed was determined and filtered samples were acidified and analysed for calcium and silicon by ICP-AES. This procedure was repeated on 17 occasions over the course of a 12 month period, to ensure that a minimum total leaching ratio of 2 $m^3\ kg^{-1}$ was achieved for all experiments.

Experimental results

The pH and elemental analysis results for the dissolution of low C/S C-S-H gels are shown in Fig. 3 (the pH data are also shown in Fig. 2, for comparison with earlier results obtained by the same method). The leaching data show that the incongruent dissolution observed in high calcium-silicon ratio gels also occurs in those of low

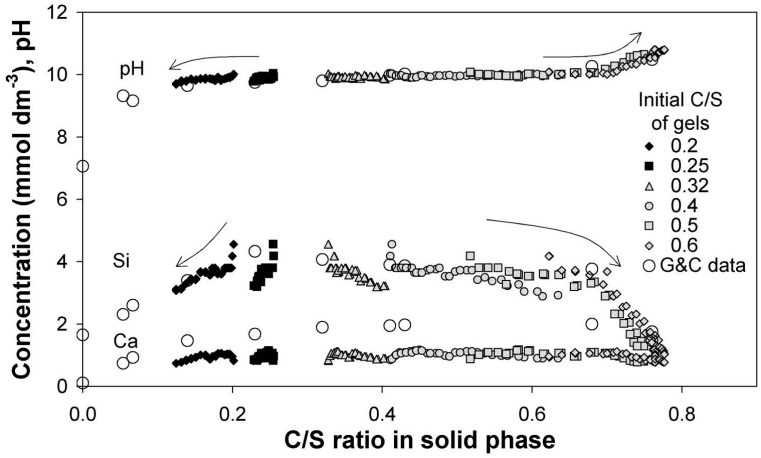

FIG. 3. Dynamic leach test results for C-S-H gels with initial C/S of 0.2 to 0.6 and comparison with reported data for single equilibrations (G&C data taken from Greenberg and Chang, 1965); arrows indicate evolution of solid composition during successive equilibrations with deionized water.

calcium/silicon ratio. For the new systems studied, the C-S-H gels with a C/S above 0.29 show preferential leaching of silicon leading to an increase in C/S. This proceeds until congruent dissolution is achieved at a ratio around 0.8. For gels with very low C/S (below 0.29), calcium is leached preferentially leaving an increasingly silica-rich gel. The reason for the divergent behaviour for gels above and a below this solid C/S value is simply related to the solution C/S. For all gels studied the solution ratio is close to 0.29 in the early stages of leaching. The observed evolution of the solid C/S is a direct consequence of the solution C/S value. Overall, the pH, calcium and silicon concentrations show little dependence on the C/S of the solid in the region $0.2 < C/S < 0.7$, other than a general decrease in silicon concentrations in the early results. Above C/S = 0.7, the pH increases, and the silicon concentration falls, as the point of congruent dissolution is approached.

The XRD data for the lowest C/S (0.2) and highest C/S (0.6) C-S-H gels after curing and drying over silica gel are shown in Fig. 4. The more-crystalline peaks observed resemble the diffraction pattern for C-S-H (I), a poorly crystalline calcium silicate hydrate phase, which is described as an imperfect version of 1.4 nm tobermorite (Chen *et al.*, 2004). For the low C/S gel, the presence of the amorphous hump centred around 20º to 25º indicates the presence of amorphous silica in addition to C-S-H (I).

Interpretation of results

The C-S-H gel dissolution data confirm that the point of congruent dissolution at around C/S = 0.8 is approached from below (i.e. for C-S-H gels with initial C/S <0.8), as well as from above. For the highest C/S C-S-H gels, the final C/S value in the aqueous phase is close to that of the solid. Overall the data are in good agreement with results obtained from single equilibration experiments (Greenberg and Chang, 1965); the main difference is the higher reported calcium concentrations (see Fig. 3).

Initial attempts to model the leaching behaviour have shown that the main features of the experimental results can be reproduced either using a two-phase model based on amorphous silica and a fixed C/S C-S-H phase or, more accurately, by applying a ideal solid solution model based on an earlier approach (Kulik and Kersten, 2001), with amorphous silica and a fixed C/S C-S-H phase as endmembers. In each case, the long-term decrease observed in aqueous concentrations could be explained by a decrease in the solubility of the solid phases. However, these interpretations are dependent on the aqueous phase having reached equilibrium with the C-S-H gel in its current state of evolution, during each leaching step. The relatively short equilibration times allowed during each step of the dynamic leach tests may not have allowed this. Further model development for C-S-H gel dissolution will therefore be carried out once data from the

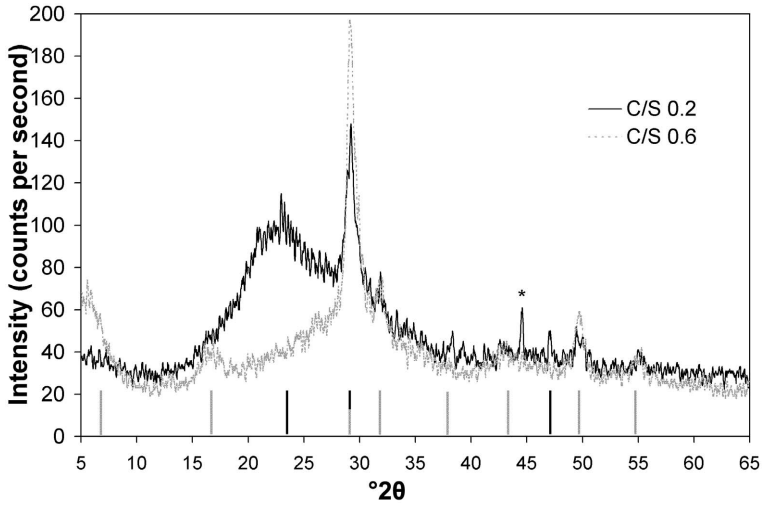

FIG. 4. X-ray diffraction patterns for C-S-H gels with C/S of 0.2 and 0.6; grey vertical lines show the peak positions for C-S-H (I) above 50% relative intensity; black vertical lines are for $CaCO_3$; * this peak is probably an artefact of the sample holder.

remainder of the experimental study are available, including: (1) further data from the sequential leaching of the C-S-H gels studied; (2) further data from longer-term C-S-H gel equilibrations; (3) final (and more accurate) determination of C/S in the C-S-H gel based on sampling and direct measurement of the solid phase; (4) XRD data for the final gels on completion of the leaching studies.

Model for package-scale and vault-scale pH performance

A spreadsheet model was developed (Heath *et al*., 2011) to help evaluate the impact of packaged wastes and groundwater composition on the maintenance of the near-field pH. It was developed specifically for NRVB (Nirex, 1997), a high-calcium backfill prepared from Ordinary Portland Cement, limestone flour and lime. The spreadsheet is designed to investigate: (1) the backfill requirement to meet a specified pH performance criteria for a vault of specified type (or for the whole disposal facility); or (2) the effects of particular waste streams and packaging concepts on the local (package-scale) pH buffering, and to compare these results with vault-averaged calculations

The vault-scale calculations consider all the NRVB in a vault and its potential reactions with major waste components, encapsulants and container materials. The amounts of each of these materials are calculated from the inventory as averaged values, for the selected vault type. The package-scale calculations consider only the local NRVB and its reactions with materials associated with the specified package and waste stream. The total volumes of NRVB plus waste considered are of the order of 400,000 m^3 for the vaults, and range from 2.6 m^3 to 48 m^3 for the various package types. For direct comparison of the vault-scale and package-scale results, the package scale volumes, amounts and porewater flow rates are scaled up to that of the vault scale (i.e. effectively considering a vault filled with a single waste package type). In each case the spreadsheet can be applied to predict the pH buffering times for a fixed volume of backfill, or to predict the volume of backfill required to provide the specified pH buffering for a fixed duration. The pH buffering stages considered are pH >12, based on the period of buffering by calcium hydroxide (but allowing for variations in the equilibrated pH with groundwater composition), and pH >9, maintained by equilibration with C-S-H phases and/ or the products of groundwater reactions with the backfill.

The spreadsheet has been set up with component models so that it can be readily updated for changes to the design, inventory or groundwater composition.

Model description and assumptions

The spreadsheet model includes: (1) the volume of backfill associated with a given vault or package type (selected from relevant design documentation); (2) the volumes of waste encapsulation grouts (selected from relevant design documentation, for vault-scale calculations, or specified by the user for package-scale calculations); (3) the volume of polymer encapsulants (specified by the user); (4) the amount of each waste component expected to react with the calcium hydroxide component of the backfill (selected from relevant inventory documentation for vault-scale calculations, or specified by the user for package scale calculations); (5) the reaction stoichiometry between each waste component and calcium hydroxide (specified by the user); (6) a set of model groundwater parameters for the calculation of the duration of pH buffers for four illustrative groundwater compositions (to reflect a range of possible salinities and host rock types as summarized in Table 1, and based on available sets of data); (7) an adjustable volumetric groundwater flow rate.

There is considerable uncertainty regarding the kinetics of many potential chemical reactions between the waste and the backfill and, consequently, in the extent of these reactions over the specified periods of pH buffering. The spreadsheet, therefore, applies simplifying assumptions based on a two-step model. In step 1, all identified reactions of the backfill with the waste and waste encapsulants are conservatively assumed to occur instantaneously and to go to completion, following saturation of the vaults by groundwater. The identified classes of reactions are discussed below. The amount of backfill consumed by these reactions is calculated within the spreadsheet. In step 2, reaction of the remaining backfill with the groundwater is considered and the relevant pH-buffering periods are calculated.

For each of the four selected groundwater compositions, a series of chemical calculations had previously been performed to calculate the evolution of pH as a function of the volumetric groundwater flow through the vault, or local package region. These calculations applied a simple one box model in which the backfill reacts with components of the inflowing groundwater. The backfill was represented as calcium hydroxide and C-S-H phases, and the formation of secondary minerals was allowed. Each set of results was fitted to an analytical form of the pH evolution in which the volume of groundwater required to lower the pH below the specified levels was plotted as a function of the C/S of the backfill.

A simplified model based on these analytical forms is included in the spreadsheet for each groundwater composition. Detailed results of the groundwater calculations and discussion of the model assumptions are given elsewhere (Heath and Hunter, 2011; Heath *et al*., 2011). The secondary minerals considered in the reaction

TABLE 1. Compositions of groundwaters applied in reactive transport calculations performed in the development of the pH buffering spreadsheet (from Heath *et al*., 2011).

Element	Elemental concentrations (mol dm^{-3})			
	Sellafield saline	Dounreay non-saline	Dounreay saline	Bure clay
	(RCF3 DET5)	(DET 6)	(DET 8)	
Ca	2.9×10^{-2}	8.9×10^{-5}	4.8×10^{-2}	1.5×10^{-2}
Mg	5.7×10^{-3}	3.3×10^{-5}	6.8×10^{-4}	1.4×10^{-2}
Na	3.7×10^{-1}	8.4×10^{-3}	8.2×10^{-2}	3.2×10^{-2}
K	4.4×10^{-3}	3.8×10^{-5}	2.5×10^{-4}	7.1×10^{-3}
Al	1.7×10^{-6}	4.6×10^{-7}	5.4×10^{-8}	7.4×10^{-9}
Sr	2.0×10^{-3}	2.0×10^{-5}	9.9×10^{-4}	1.1×10^{-3}
Si	2.5×10^{-4}	1.1×10^{-4}	7.6×10^{-5}	9.4×10^{-5}
Cl	4.2×10^{-1}	5.3×10^{-3}	1.7×10^{-1}	3.0×10^{-2}
C	1.0×10^{-3}	2.8×10^{-3}	1.7×10^{-4}	2.1×10^{-3}
S	1.2×10^{-2}	2.8×10^{-4}	6.3×10^{-3}	3.4×10^{-2}
pH	7.22	8.75	7.73	7.10

Carbon concentration is for carbonates only; sulfur concentration is for sulfates only.

between the backfill and the groundwater are calcite and brucite. Although brucite may undergo further reactions with other components of the backfill, this is not expected to further reduce the buffering capacity.

Where a backfill-consuming reaction involves reactants both from the waste and the groundwater, the predicted duration of the pH buffer may depend on the amount of groundwater component accumulated in the buffering period. An iterative approach is therefore required. The spreadsheet allows such an approach to be applied for ettringite formation, which involves aluminium from the backfill and encapsulation grouts and sulfate predominantly from the groundwater. In the spreadsheet model, ettringite is the only solid phase treated in this manner (others are either considered as step 1 reactions between backfill and waste components or step 2 reactions included in the groundwater modelling). Alternative models with different assumptions about the solid phases formed are possible, but the important point is to ensure that each reactive component of the waste or groundwater is accounted for, but not duplicated by inclusion of additional similar solid phases.

In assessing package-scale performance for conditioned waste from a particular waste stream, the predicted pH performance is compared with the vault-averaged results by calculating the ratio of pH buffering times. Many of the model assumptions are common to both the vault-scale and package-scale so that the effect of any uncertainties associated with these assumptions will be cancelled out by this approach.

Reactions affecting pH performance

For the package-scale calculations, the reactions of encapsulants and waste stream components with the backfill need to be added by the spreadsheet user. These wide ranging processes fall into a number of classes, represented by the net forward reactions outlined below.

Pozzolanic reaction with encapsulation grouts of low C/S:

e.g. $Ca(OH)_2(s)$ + C-S-H (lower C/S) → C-S-H (higher C/S)

partial degradation of organic materials:

e.g. $RCOOR' + 0.5Ca(OH)_2(s) \rightarrow RCOO^- + R'OH + 0.5Ca^{2+}$

complete degradation of cellulose-like organic waste components:

e.g. $C_6H_{10}O_5 + 3Ca(OH)_2(s) \rightarrow 3CO_3^{2-} + 3CH_4(g) + 2H_2O + 3Ca^{2+}$

reaction with reactive metals:

e.g. $U(s) + 4H_2O \rightarrow UO_2(OH)_2(s) + 3H_2(g)$

conversion of metal oxides and hydroxides to mixed calcium-metal solids

e.g. $2UO_2(OH)_2(s) + Ca(OH)_2(s) \rightarrow CaU_2O_7(s) + 3H_2O$

hydroxide formation from metal salts:

e.g. $Mg^{2+} + Ca(OH)_2(s) \rightarrow Mg(OH)_2(s) + Ca^{2+}$

reaction of protonated forms:

e.g. $HCO_3^- + 0.5Ca(OH)_2(s) \rightarrow 0.5Ca^{2+} + CO_3^{2-} + H_2O$

reaction of unprotonated anions:

e.g. $5Ca(OH)_2(s) + 3PO_4^{3-} \rightarrow Ca_5(PO_4)_3OH(s) + 9OH^-$

reaction of silicates and aluminosilicates:

e.g. $Na_6[(AlO_2)_6(SiO_2)_{30}]\cdot 24H_2O + Ca(OH)_2(s) \rightarrow$ C-S-H + calcium aluminate + $6Na^+$

formation of higher aqueous hydrolysis species:

e.g. $Fe(OH)_3(s) + 0.5Ca(OH)_2(s) \rightarrow Fe(OH)_4^- + 0.5Ca^{2+}$

The pozzolanic reaction between the backfill and the cementitious grouts generally leads to the consumption of calcium hydroxide component of the backfill and a reduction in the period of buffering above pH 12. However, the products of such reactions (e.g. C-S-H phases) may themselves contribute to the lengthening of the later-stage pH buffering at pH >9. The spreadsheet allows the long-term effects of the pozzolanic reaction products either to be included or excluded from the calculation. It is noted that the reaction of reactive metals does not generally result in the consumption of calcium hydroxide. However, onward reaction of the resulting oxide or hydroxide of the metal may do so (as indicated above for uranium).

Model results

The model has been applied to vault-scale and disposal-facility-scale calculations to investigate the expected duration of pH buffering phases. For

the specified design, waste inventory and selected groundwater type (Sellafield saline), and given the various assumptions (Heath and Hunter, 2011), periods of pH buffering at pH >9 above one million years were generally calculated, for the vault scale. In one scenario, where peripheral backfill (around the edges of the vaults) was excluded from the calculation, and no credit was taken for buffering provided by the products of the pozzolanic reaction, the predicted period of pH >9 buffering for unshielded ILW vaults was around 1.06 million years (only slightly higher than the period of required buffering performance).

Application of this model is illustrated by its use to estimate the effects of the waste packages from three waste streams (Nuclear Decommissioning Authority, 2011) on the alkaline buffering performance of the near field (Heath *et al*., 2011): (1) encapsulated barium carbonate slurry/MEB crud (waste stream identifier 2F06; MEB denotes multi-element bottles, used for spent fuel storage); (2) a steel decommissioning waste (waste stream identifier 9D311); and (3) plutonium-contaminated materials (waste stream identifier 2D03).

In each of these cases, the predicted duration of the pH >9 buffer was greater than that calculated for the vault-averaged results (Table 2) for the same sets of assumptions. This suggests that these waste streams will cause no additional post-closure pH effects above those of the inventory as a whole. However, for the plutonium-contaminated material (PCM) the period of pH >12 buffering was reduced compared with the vault-averaged result.

Calculations in which the groundwater type was varied showed a strong dependence of the predicted buffering times on water composition. Most significantly, groundwater with high carbonate and magnesium concentrations showed reduced pH buffering periods (above pH 12), although for magnesium the longer term buffer (above pH 9) was extended. Groundwaters with lower calcium and silicon concentrations or with higher ionic strengths resulted in more rapid backfill dissolution and reduced pH buffering periods. Buffering at pH >12 is decreased due to ettringite formation for all waters. The extent of this effect increases with sulfate concentration until the ettringite formation becomes limited by the amount of aluminium in the waste and backfill. The predicted buffering periods are inversely proportional to the groundwater flow rate, and consequently can be greatly extended for concepts based on geologies with lower flow rates (e.g. clays).

Conclusions

The UK cementitious disposal concept for ILW and some LLW requires the long-term maintenance of alkaline near-field conditions to

TABLE 2. The pH performance spreadsheet results for selected waste streams: ratio of pH buffering time for waste package to vault-averaged result.

Model selections			
Waste stream	$BaCO_3$/MEB crud	Steel decom. waste	PCM
Identifier	2F06	9D311	2D03
Package type	500 l drum	4 m box	500 l annular drum
Vault type	unshielded ILW	shielded ILW/LLW	unshielded ILW
Groundwater type	Sellafield saline	Sellafield saline	Sellafield saline
VF(package)/ m^3 $year^{-1}$	8.7×10^{-4}	6.5×10^{-3}	8.5×10^{-4}
VF(vault)/ m^3 $year^{-1}$	25.2	11.4	25.2
Model results			
R(pH>12)	2.7	3.7	0.5
R(pH>9)	2.3	1.8	1.2

R(pH>12) is the ratio of the predicted pH buffering time above pH 12 for the given package to the equivalent vault-averaged quantity;
R(pH>9) is the corresponding ratio based on predicted buffering times at pH >9.
VF(vault) is the volumetric groundwater flow rate through the vault;
VF(package) is the volumetric groundwater flow rate through the package region (including local backfill).

provide a chemical barrier to the migration of many radionuclides. Demonstration of the required pH buffering performance depends on an understanding of (1) the mechanisms by which the backfill chemically conditions the groundwater; and (2) the reactions of the backfill with the groundwater, waste and other repository components. The ongoing development and application of such understanding has been illustrated with: (1) results from an ongoing investigation of the leaching behaviour of C-S-H gels and associated structural changes to the C-S-H phases of relevance to long-term pH evolution; and (2) the development and application of a spreadsheet model to asses the vault-scale and package-scale pH performance, including the effects of all identified reactions.

The C-S-H gel results confirm that a congruent dissolution point around C/S = 0.8 is approached by leaching from below (i.e. for gels with $0.29 < C/S < 0.8$), as well as from above, as reported elsewhere.

Acknowledgements

The work reported here was funded by the Nuclear Decommissioning Authority Radioactive Waste Management Directorate. Professor F.P. Glasser (University of Aberdeen), Dr A.R. Hoch (AMEC) and S. Magalhaes (formerly Serco) are thanked for helpful discussions and advice. Dr C. Utton (University of Sheffield) is thanked for providing the X-ray diffraction measurements.

References

Chambers, A.V., Heath, T.G., Hunter, F.M.I. and Manning, M.C. (2003) *The Effect of Sodium Chloride on the Dissolution of Calcium Silicate Hydrate Gels.* Serco Assurance Report, SA/ENV-0623.†

Chen, J.J., Thomas, J.J., Taylor, H.F.W. and Jennings, H.M. (2004) Solubility and structure of calcium silicate hydrate. *Cement Concrete Research*, **34**, 1499–1519.

Greenberg, S.A. and Chang, T.N. (1965) Investigation of the colloidal hydrated calcium silicates. II. Solubility relationships in the calcium oxide–silica–water system at 25ºC. *Journal of Physical Chemistry*, **69**, 182–188.

Harris, A.W., Manning, M.C., Tearle, W.M. and Tweed, C.J. (2002) Testing of models for the dissolution of cements – leaching of synthetic C-S-H gels. *Cement and Concrete Research*, **32**, 731–746.

Heath, T.G. and Hunter, F.M.I. (2011) *Calculation of near-field pH buffering: Effect of polymer encapsulant.* Serco Assurance Report, SA/ENV-0909.

Heath, T.G., Hunter, F.M.I., Magalhaes, S. and Smith, V. (2011) *Spreadsheet model for the impact of waste packages on local pH conditioning*. Serco Report, SERCO/TAS/E000356/01, Issue 1.†

Hoch, A., Glasser, F., Baston, G.M.N. and Smith, V. (2009) *Modelling pH evolution in the near field of a cementitious repository*. TOUGH Symposium, Lawrence Berkeley National Laboratory, Berkeley, California, 14–16 September 2009.

Hoch, A.R., Baston, G.M.N., Glasser, F.P., Hunter, F.M.I. and Smith, V. (2012) Modelling evolution in the near field of a cementitious repository. *Mineralogical Magazine*, **76**, 3055–3069.

Kulik, D.A. and Kersten, M. (2001) Aqueous solubility diagrams for cementitious waste stabilisation systems: II. End-member stoichiometries of ideal calcium silicate hydrate solid solutions. *Journal of the American Ceramic Society*, **84**, 3017–3026.

Nirex (1997) *Development of the Nirex Reference Vault Backfill: Report on Current Status in 1994*. Nirex Science Report, S/97/014.†

Nuclear Decommissioning Authority (2010*a*) *Geological Disposal: Generic Post-closure Safety Assessment*. Nuclear Decommissioning Authority Report, NDA/RWMD/030.†

Nuclear Decommissioning Authority (2010*b*) *Geological Disposal. Near-field Evolution Status Report*. Nuclear Decommissioning Authority Report, NDA/RWMD/033.†

Nuclear Decommissioning Authority (2011) *Geological Disposal: An Introduction to the Derived Inventory*. Nuclear Decommissioning Authority Report, NDA/RWMD/065.†

Swanton, S.W., Fairbrother, H.J. and Turner, N.A. (2004) *The Effect of Sodium Chloride on the Dissolution of Calcium Silicate Hydrate Gels. II. Effects of Temperature and Cation Type*. Serco Assurance Report, SA/ENV-0725.†

Wang, L., Martens, E., Jacques, D., De Cannière, P., Berry, J.A. and Mallants, D. (2009) *Review of sorption values for the cementitious near field of a near surface radioactive waste disposal facility, project near surface disposal of category A waste at Dessel*. ONDRAF/NIRAS Report, 5-03-03, version 1.

† The technical reports indicated are available from the Nuclear Decommissioning Authority website at http://www.nda.gov.uk/documents/biblio/.